Low-pressure corona textures between olivine and plagioclase in unmetamorphosed gabbros from Black Hill, South Australia

SIMON P. TURNER* AND KURT STÜWE

Department of Geology and Geophysics, University of Adelaide GPO Box 498, Adelaide, South Australia 5001

Abstract

Olivine–plagioclase corona textures occur in ophitic to sub-ophitic olivine gabbros at Black Hill, South Australia. Contrasting with many corona and symplectite textures previously described, these do not involve spinel or garnet as reaction products and did not form under high-pressure conditions. Rather, the coronas formed at no more than 1 kbar pressure and are composed of a shell of orthopyroxene around the olivine often succeeded by a shell of amphibole or occasionally biotite. Beyond this, a vermicular symplectite of anorthite containing orthopyroxene and rarer amphibole vermicules extends out to host plagioclase of labradorite composition. Textural relations are used to infer a subsolidus igneous origin for all but the orthopyroxene shell which may have formed in the presence of some magma. Compositional zonation is absent from all the constituent phases except the amphibole shell which is strongly zoned in Mg# and may have a late origin. An average maximum corona width of 150–200 μm indicates a limiting distance for subsolidus chemical diffusion. The corona products involve the reactants olivine and plagioclase in the proportions 1:3 and symplectite formation may have been promoted by a Na potential gradient. The system must also have been open to minor components including H_2O and TiO_2, with H_2O possibly being derived from a hydrothermal system. Such systems may have been set up in the country rocks on intrusion of the magma and subsequently collapsed inwards into the pluton during sub-solidus cooling.

KEYWORDS: olivine-plagioclase, corona, symplectite, low pressure.

Introduction

REACTION coronas between olivine and plagioclase are a common feature of many gabbroic rocks. In general, such coronas formed at high pressures and are associated with garnet and/or spinel plus clinopyroxene as reaction products (see Nishiyama, 1983 for a review). Coronas are usually described from metamorphosed gabbros and consequently have often been interpreted to be associated with protracted cooling during the metamorphic event (e.g. Mongkoltip and Ashworth, 1983). However, there has been some considerable debate over this metamorphic versus igneous origin (e.g. Joesten, 1986 *a* and *b*; Ashworth, 1986).

Here we report on new symplectitic reaction coronas between olivine and plagioclase in gabbroic rocks from Black Hill, South Australia. The gabbroic rocks at Black Hill (about 85 km E of Adelaide) intruded at relatively low pressures after the end of regional metamorphism and have not experienced any metamorphism subsequently and are thus pertinent to the debate mentioned above. The physico-chemical conditions during corona formation are not only different from many of those described in the literature, but their formation is well constrained by the conditions during crystallisation of the magma as the coronas must have formed during initial igneous cooling.

Geological setting

Undeformed layered gabbroic plutons outcrop along the eastern margin of the Adelaide Foldbelt in South Australia. The plutons yield early Ordovician (489 Ma) crystallization ages (Turner, 1992) consistent with intrusion just after the end

* Present address: Department of Earth Sciences, Open University, Milton Keynes, MK7 6AA, England.

Mineralogical Magazine, December 1992, Vol. 56, pp. 503–509

of the Cambro-Ordovician Delamerian Orogeny that formed the foldbelt. At Black Hill, the rocks have similar whole-rock compositions to many previously described corona-bearing gabbroic rocks. Mineralogical and geochemical investigations (Turner, 1992) show that the plutons formed by shallow (<1 kbar) isobaric crystallization of a typical continental tholeiitic magma. Accordingly, the sequential appearance of the phases olivine (ol), plagioclase (pl), two pyroxenes (opx and cpx), magnetite and alkali feldspar between 1200 and 900 °C produced a series of layered peridotites, troctolites, olivine gabbros, gabbronorites and potassic gabbronorites. Water contents are deduced to be moderate (2–3%) and fractionation combined with assimilation led to the stabilization of biotite in the potassic gabbronorites (Turner, 1992). With the exception of these potassic gabbronorites and separate hydrated 'coarse zones', related to post solidification, inward collapse of a hydrothermal system, most of the gabbros consist primarily of anhydrous phases with minor development of amphibole (amph) at the rims of pyroxenes.

Description of the symplectites

The symplectites described here occur in ophitic to sub-ophitic olivine gabbros with the assemblage and averaged volumetric mineral abundances of olivine (6%) + plagioclase (44%) + orthopyroxene (16%) ± clinopyroxene (26%) ± magnetite (2%) ± amphibole (5%) ± biotite (1%). Simpler coronas of orthopyroxene around olivine occur in troctolites (olivine 39%, plagioclase 47%, orthopyroxene 1%, clinopyroxene 7%, amphibole 4%, magnetite 2%) where pyroxene is an incoming liquidus phase. Following the order of fractional crystallisation, olivine and plagioclase are near euhedral and cumulate with an average grainsize of 1–2 mm, whereas pyroxene forms intercumulate ophitic to sub-ophitic grains which may reach 4 mm in diameter. In many of the olivine-bearing rocks, particularly the troctolites, orthopyroxene forms thin rims (10–15 μm) between olivine (Fo_{82-75}) and plagioclase (An_{64}). Such reaction coronas are common to many olivine and plagioclase-bearing igneous rocks (e.g. Nishiyama, 1983) and can be ascribed to an increase of silica activity during the fractional crystallisation following the reaction:

$$\text{ol} + SiO_2 \Rightarrow \text{opx} \qquad (1)$$

The activity of silica during this reaction was determined from ol–opx equilibria (Campbell and Noland, 1974) to be: $-\log a_{SiO_2} = 0.13–0.16$. It seems likely that this reaction occurs in the presence of some melt and this is supported by textures in the more anhydrous troctolites in which the orthopyroxene rim is seen to invade the margins of olivine grains (crystallized prior to the opx-rim) but not the surrounding plagioclase laths (inferred to have crystallized subsequently).

However, in some of the more hydrous (usually hornblende-bearing) olivine gabbros, multiple reaction coronas involving symplectites formed between olivines (Fo_{74}) and plagioclase (An_{64}). These multiple corona textures are formed at both contacts with plagioclase in the matrix, and contacts with plagioclase inclusions within olivine, but they are not developed at the olivine-pyroxene contacts (Fig. 1*a–f*). They are cored by olivine which is rimmed by an inner shell of orthopyroxene usually followed by a second shell of amphibole or, more rarely, biotite. However, this hydrous second shell is not ubiquitous and some corona structures contain no hydrous shell (Fig. 1*f*). These two one-phase shells are typically mantled by an outer shell consisting of a wide zone of a two or three phase vermicular symplectite. This third, vermicular, shell clearly impinges on, or grows into the host plagioclase grains (Fig. 1*a*). Symplectites involving spinel as a product phase are also observed (e.g. Fig. 1*e*) but usually form islands within olivine grains and represent later oxidation features in which olivine degrades to orthopyroxene with magnetite exsolution.

The inner orthopyroxene shell (En_{76}) is generally of a consistent width of 10–15 μm and is only mildly zoned with the tschermakite component of the orthopyroxene generally increasing with distance from olivine (Table 1). The following shell of amphibole is also 10–15 μm wide and is strongly zoned from SiO_2-rich, Al_2O_3-poor, Mg# 82 (Mg-hastingsite) adjacent to the orthopyroxene to SiO_2-poor, Al_2O_3-rich, Mg# 76 (pargasite) at the boundary with anorthite. The boundary between the orthopyroxene and amphibole shells is not regular but scalloped and embayed sometimes all the way to the olivine core (Fig. 1*c*) so that amphibole olivine contacts are formed. Occasionally the orthopyroxene shell is almost entirely absent with only remnants and small islands of orthopyroxene remaining within the amphibole.

The symplectitic part of the three shell corona texture is grown to a diameter up to 150–200 μm. It consists of anorthite (An_{90-86}) containing elongate vermicules of orthopyroxene (En_{74-72}) and often minor amphibole (Fig. 1*a–f*, Table 1) with the vermicules being generally arrayed in a radial fashion pointing outwards from the olivine in the corona core. When they occur, the rarer (<20%) amphibole vermicules are concentrated at the inner part of the symplectite near the

amphibole shell, whereas the more dominant orthopyroxene vermicules are distributed across the whole symplectite. Local compositional (and optical) disequilibrium occurs at the outer boundary between the anorthitic plagioclase (An_{86}) of the symplectite and the plagioclase it impinges upon, which is labradorite (An_{70-63}) typical of these olivine gabbros. This third shell is not ubiquitous and in the same thin section olivines may develop just the first, opx, shell; both the opx and amphibole shell; or, most commonly, all three. There is no vermicular symplectite formed between olivine and plagioclase that are separated by orthopyroxene over distances greater than 300 μ.

Table 1 gives microprobe analyses for a traverse across the corona shown in Fig. 1*a–c*. For this corona the constituent product phases occur in the proportions orthopyroxene shell 13%, amphibole shell 16%, plagioclase of symplectite 57%, orthopyroxene vermicules in symplectite 11%, amphibole vermicules in symplectite 3%. The following estimates of the conditions of corona formation coincide with likely conditions for solidification of the plutons as a whole. Temperature from amphibole–plagioclase thermometry in the corona texture (Blundy and Holland, 1990): ~980 °C (Note that Helz, 1982, places the amphibole-in basalt solidus crossover at 900 °C at 1 kbar). Pressure from CATS geobarometer (Ellis, 1980): 0.5–0.8 kbar.

A generalized net reaction for the coronas can be written:

$$\text{ol} + \text{pl} + H_2O \Rightarrow \text{opx} + \text{an} \pm \text{amph} \quad (2)$$

in which Si, Na and Al must be removed from plagioclase to the olivine to produce orthopyroxene and amphibole. This net extraction leaves a residual host plagioclase which is more Ca and Al-rich than the reactant plagioclase.

Discussion

The multiple corona textures described above formed in an at least 7-component system involving the components SiO_2, Al_2O_3, FeO, MgO, CaO, Na_2O and H_2O. The number of phases involved in the texture, on the other hand, appears to be no larger than 4 (olivine, orthopyroxene, amphibole, plagioclase) and the corona-forming reaction is of a high thermodynamic variance. It is therefore extremely difficult to interpret the reaction-forming processes on the basis of phase diagrams. Here, we rely on detailed textural observations and the descriptions above to constrain some of the corona-forming conditions and processes.

Clearly, the coronas reflect the growing instability of the olivine–plagioclase equilibrium also reflected by the complete absence of olivine in the more evolved gabbronorites. In some olivine gabbros the original presence of olivine can only be inferred from the occurrence of coronas which no longer contain any olivine core. It is an important point that the full coronas are not developed in the troctolites which in terms of their bulk chemistry are not greatly different to the olivine gabbros. In the troctolites only the orthopyroxene shell is formed and there is textural evidence suggesting that the orthopyroxene shell formed above the solidus by reaction with melt (see above). Subsequently increasing a_{H_2O}, thought to be important in symplectite growth, would enlarge the stability field of olivine with respect to orthopyroxene (e.g. Kushiro, 1969) and therefore not favour the formation of orthopyroxene rims.

In the olivine gabbros, amphibole and symplectite shells are formed in addition to the orthopyroxene shell. This change from coronitic to vermicular textures might be interpreted as an indicator for a distance beyond which diffusion became too restricted for broad reaction front migration. However, the plagioclase in the symplectite is near pure anorthite and is a second, new reaction product now being produced together with opx. Textural evidence, in which the symplectites impinge on, or grow into plagioclase grains (Fig. 1*d*), or along plagioclase–plagioclase grain boundaries, argues strongly for a sub-solidus origin of the symplectitic part of the texture. Additionally, corona textures are formed around plagioclase inclusions within olivine but they are not developed at the olivine–pyroxene contacts. Fig. 1*a* shows cumulus grains of olivine and plagioclase that must have crystallized prior to the intercumulus augite they are both included within. A multiple corona is developed at boundaries between the olivine and plagioclase but not at olivine–augite boundaries (though note in Fig. 1*b* that a thin orthopyroxene rim exists between the olivine and the augite consistent with an above-solidus formation for orthopyroxene). This also suggests a sub-solidus origin as the grain boundaries must have been fixed prior to corona growth. We therefore suggest that the addition of a second product phase in the outer, vermicular corona balances the vanishing of melt as part of the reactant assemblage in order to maintain the variance of the reaction. The absence of symplectite coronas at olivine–augite boundaries reflects a greater chemical stability between olivine and augite than between olivine and plagioclase (augite is, at most, rimmed by amphibole).

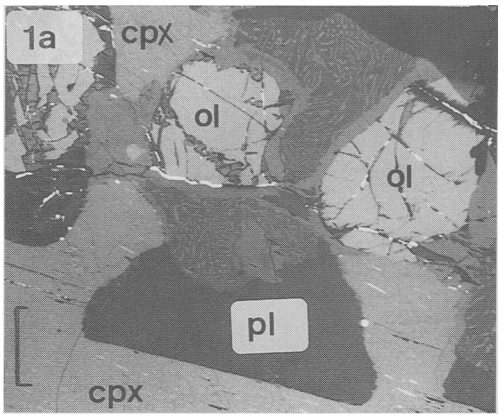
1a
cpx
ol
ol
pl
cpx

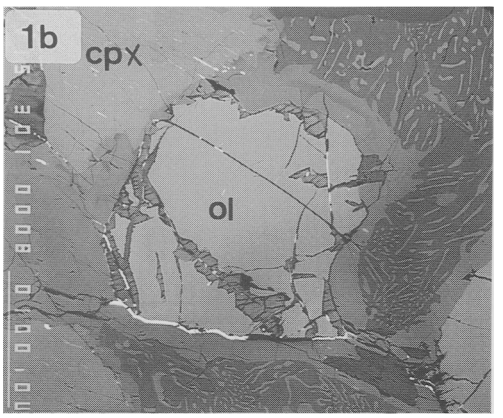
1b
cpx
ol

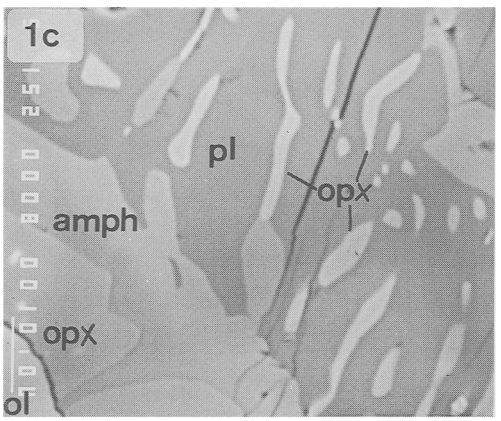
1c
pl
opx
amph
opx
ol

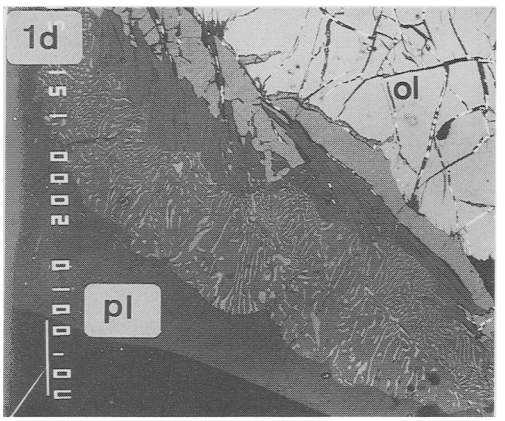
1d
ol
pl

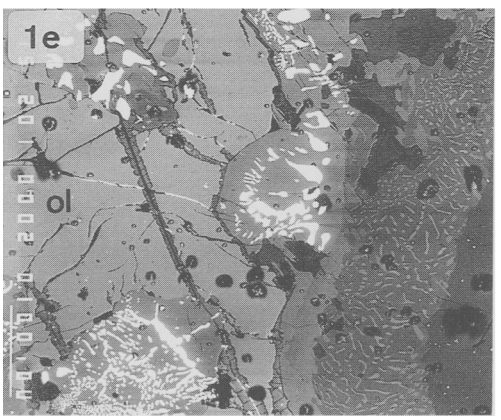
1e
ol

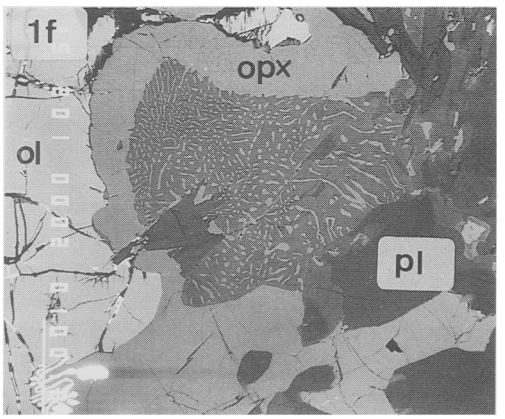
1f
opx
ol
pl

The observation that some coronas consist of just the orthopyroxene rim followed by a symplectite of anorthite containing orthopyroxene vermicules requires equation 2 to be written without amphibole. Increasing the anorthite component of the plagioclase frees SiO_2 for reaction with olivine to produce orthopyroxene, however, this can be balanced only by loss of Na:

$$2x \text{ pl} + 6 \text{ ol} \Rightarrow 12 \text{ opx} + 2(x\text{-}x^2) \text{ an} + x^2 \text{ Na-fluid} \quad (3)$$

where x is the mol fraction of albite in plagioclase which is about 0.35 in the case considered here. If this is correct then the driving mechanism for symplectite formation may have been a potential gradient in Na during subsolidus cooling.

The reason for the sub-solidus anorthite–orthopyroxene symplectite formation in the olivine gabbros but not in the troctolites remains somewhat obscure, though the troctolites have a more cumulate texture and the removal of intercumulus liquid may have resulted in an absence of components, including volatiles, necessary for symplectite growth. In particular a certain critical H_2O component may be required for the full corona formation as, at magmatic temperatures, plagioclase stability is decreased by increasing p_{H_2O}. Inward collapse of a hydrothermal system, set up in the country rocks, shortly after solidification of the plutons is thought to have produced localized 'coarse zones' where the gabbros become completely uralitized (Turner, 1992). We suggest that this may also have promoted diffusion and growth of the complete multiple textures. This is supported by detailed compositional mass balance analysis of anorthite-orthopyroxene symplectite growth (van Lamoen, 1979; Nishiyama, 1983; and Mongkoltip and Ashworth, 1983) indicating diffusive growth under conditions where several components have restricted diffusion ranges.

The development of the amphibole shell is interpreted to post-date the main symplectite formation, following the reaction:

$$10 \text{ opx} + 7 \text{ an} + 2 \text{ } H_2O \Rightarrow 2 \text{ amph} \quad (4)$$

and may be related to a general hydration of the pyroxene margins seen in the gabbros at Black Hill (note from Table 1, the anorthite contains sufficient Na to balance the amphibole). This is indicated by the occurrence of coronas that lack amphibole rims (e.g. Fig. 1*f*) and the textural evidence that, where it does occur, amphibole is replacing orthopyroxene and the outer symplectite. In Fig. 1*c* amphibole appears to be migrating into the orthopyroxene shell, in places reaching right to the olivine core, whilst on the other side it is seen migrating up orthopyroxene vermicules in the symplectite and elsewhere replacing them. The conspicuous compositional zoning in the amphibole (Fig. 1*c*, Table 1) supports this notion with half of the shell on the orthopyroxene side being Al_2O_3 poor and Mg-rich whilst the other half is Al_2O_3-rich and Mg-poor. The mid-point between these two halves is taken to be the original orthopyroxene-symplectite boundary.

Mass balance calculations can be used to see if the bulk composition of the three shell corona can be expressed in terms of the two reacting components. The relative volumes of each reaction product component (estimated above for the corona in Fig. 1*b*) were calculated by integrating the area of each phase on probe photographs. The bulk corona composition can then be estimated by multiplying the abundance of each component in each product phase by the relative volume for that phase and its density. Table 2 shows the results of least squares mixing of the host olivine and plagioclase to approximate the estimated bulk composition of the corona. The sum of residuals squared is moderately high (~9) which may partially reflect the errors in calculating the

FIG. 1. (*a–f*) Back scattered electron images of the corona textures (scale bar 100 μ in all except 1*c* 10 μm, ol = olivine; pl = plagioclase; opx = orthopyroxene; cpx = clinopyroxene; amph = amphibole). (*a*) Cumulus olivines and plagioclase enclosed within intercumulus clinopyroxene with the corona symplectite structure developed only at olivine–plagioclase boundaries indicating a subsolidus origin for the symplectite part of the corona. (*b*) Enlargement of 1*a*; note the thin orthopyroxene rim embays into the olivine and also occurs between the olivine and clinopyroxene, suggesting its magmatic origin. (*c*) Enlargement of the top portion of 1*b* showing details of the subsolidus, vermicular symplectite of anorthite containing orthopyroxene vermicules. Note that the amphibole rim appears to represent later degradation, replacing orthopyroxene in the rim around olivine and in the vermicular symplectite. (*d*) Another corona showing the impingement of the symplectite shell into the host plagioclase. Note that in this example biotite takes the place of amphibole. (*e*) An example of the unrelated coronas which occur as island within olivine grains as well as at the olivine margins in which olivine is oxidizing to orthopyroxene and spinel (titaniferous magnetite). (*f*) Two shell corona structure in which the hydrous shell is absent indicating it forms by later degradation. Note that no symplectite is formed between olivine and plagioclase in the bottom part of the photo presumably because the olivine-plagioclase distance is greater than the diffusion distances.

Table 1: Electron microprobe analyses of from the symplectite shown in figures 1a-f.

phase	ol-1	ol-2	ol-3	ol-4	ol-5	ol-6	opx-1	opx-2	opx-3	amph-1	amph-2	amph-3	an-1	an-2	an-3	an-4	plag-1	plag-2	opx	opx	amph	amph
location	core					rim	adj ol		adj amph	adj opx		adj an	adj amph				rim	core	vermicular lamellae in symplectite			
SiO2	38.22	38.21	38.05	37.73	37.79	38.26	54.15	53.46	53.89	48.20	45.66	42.89	44.33	44.54	45.03	44.36	51.50	50.71	54.00	53.36	43.76	45.18
TiO2	0.00	0.07	0.05	0.00	0.03	0.03	0.00	0.00	0.00	0.30	0.53	0.44	0.01	0.00	0.29	0.00	0.06	0.03	0.00	0.16	0.25	0.36
Al2O3	0.00	0.00	0.00	0.01	0.01	0.00	0.34	0.78	0.57	7.15	9.57	16.36	31.56	32.54	32.53	31.89	28.49	28.25	1.62	3.23	14.61	12.41
FeO	23.62	23.13	23.31	23.21	23.35	23.26	15.17	14.64	14.65	6.96	7.61	7.45	0.70	0.32	0.41	0.04	0.26	0.29	17.15	16.49	7.43	7.45
MnO	0.54	0.30	0.46	0.44	0.45	0.38	0.45	0.44	0.33	0.17	0.08	0.14	0.20	0.05	0.04	0.35	0.04	0.00	0.50	0.39	0.18	0.00
MgO	37.14	37.05	37.18	36.96	37.42	37.55	27.84	27.33	27.04	18.05	16.77	13.18	0.56	0.12	0.00	0.19	0.00	0.00	25.44	25.05	13.66	15.21
CaO	0.07	0.00	0.00	0.00	0.00	0.17	0.19	0.34	0.49	11.46	11.86	13.00	17.68	18.42	17.74	18.20	12.63	13.16	0.90	1.15	12.80	12.52
Na2O	0.00	0.00	0.00	0.00	0.00	0.00	0.07	0.00	0.25	1.32	1.59	2.18	1.28	1.13	1.53	1.40	4.30	4.14	0.00	0.01	1.65	1.97
K2O	0.00	0.00	0.00	0.04	0.00	0.06	0.01	0.00	0.00	0.40	0.45	0.45	0.05	0.00	0.12	0.10	0.09	0.05	0.07	0.04	0.28	0.22
Cr2O3	0.01	0.00	0.00	0.00	0.00	0.01	0.00	0.00	0.00	0.20	0.00	0.09	0.00	0.00	0.00	0.00	0.00	0.00	0.00	0.25	0.08	0.00
Total	99.60	98.76	99.05	98.38	99.04	99.72	98.22	96.98	97.23	94.21	94.10	96.16	96.36	97.12	97.67	96.53	97.37	96.63	99.68	100.13	94.70	95.32
Structural formulae based on:			4 oxygens				6 oxygens			23 oxygens			32 oxygens				32		6		23	
Si	1.0054	1.0102	1.0051	1.0039	0.9992	1.0036	1.9845	1.9804	1.9916	7.0894	6.7774	6.2537	8.5329	8.4887	8.5302	8.5204	9.6119	9.5588	1.9692	1.9326	6.4516	6.6118
Ti	0.0000	0.0014	0.0011	0.0000	0.0006	0.0007	0.0000	0.0000	0.0000	0.0329	0.0590	0.0477	0.0020	0.0000	0.0410	0.0000	0.0089	0.0038	0.0000	0.0044	0.0274	0.0392
Al	0.0000	0.0000	0.0000	0.0002	0.0003	0.0000	0.0147	0.0339	0.0246	1.2389	1.6730	2.8102	7.1580	7.3071	7.2616	7.2162	6.2665	6.2739	0.0697	0.1380	2.5385	2.1404
Fe	0.5193	0.5111	0.5146	0.5162	0.5161	0.5099	0.4648	0.4534	0.4527	0.8551	0.9447	0.9085	0.1130	0.0504	0.0651	0.0070	0.0401	0.0463	0.5228	0.4992	0.9157	0.9108
Mn	0.0121	0.0067	0.0104	0.0100	0.0100	0.0084	0.0141	0.0136	0.0104	0.0216	0.0103	0.0174	0.0320	0.0082	0.0058	0.0566	0.0068	0.0000	0.0153	0.0120	0.0226	0.0000
Mg	1.4554	1.4591	1.4627	1.4651	1.4738	1.4670	1.5200	1.5081	1.4883	3.9554	3.7073	2.8619	0.1595	0.0353	0.0000	0.0547	0.0002	0.0000	1.3820	1.3512	2.9995	3.3153
Ca	0.0021	0.0000	0.0000	0.0000	0.0000	0.0047	0.0076	0.0133	0.0193	1.8053	1.8849	2.0304	3.6446	3.7594	3.5996	3.7432	2.5241	2.6570	0.0352	0.0446	2.0208	1.9615
Na	0.0000	0.0000	0.0000	0.0000	0.0000	0.0000	0.0047	0.0000	0.0179	0.3762	0.4562	0.6153	0.4767	0.4171	0.5609	0.5217	1.5545	1.5107	0.0000	0.0009	0.4703	0.5586
K	0.0000	0.0000	0.0000	0.0013	0.0000	0.0021	0.0004	0.0000	0.0000	0.0742	0.0849	0.0827	0.0113	0.0000	0.0284	0.0251	0.0208	0.0110	0.0032	0.0016	0.0530	0.0413
Cr	0.0003	0.0000	0.0000	0.0000	0.0000	0.0002	0.0000	0.0000	0.0001	0.0231	0.0000	0.0099	0.0000	0.0000	0.0000	0.0000	0.0000	0.0000	0.0000	0.0073	0.0094	0.0000
Total	2.9946	2.9885	2.9939	2.9967	3.0001	2.9967	4.0107	4.0027	4.0049	15.4720	15.5977	15.6376	20.1301	20.0663	20.0926	20.1449	20.0337	20.0614	3.9975	3.9917	15.5087	15.5788
Mg#	0.74	0.74	0.74	0.74	0.74	0.74	0.77	0.77	0.77	0.82	0.80	0.76	0.59	0.41	0.00	0.89	0.00	0.00	0.73	0.73	0.77	0.78
Na/(Ca+Na+K)	0.00	-	-	0.00	-	0.00	0.37	0.00	0.48	0.17	0.19	0.23	0.12	0.10	0.13	0.12	0.38	0.36	0.00	0.02	0.18	0.22
Ca/(Ca+Na+K)	1.00	-	-	0.00	-	0.70	0.60	1.00	0.52	0.80	0.78	0.74	0.88	0.90	0.86	0.87	0.62	0.64	0.92	0.95	0.79	0.77
Ca/(Ca+Fe+Mg)	0.00	0.00	0.00	0.00	0.00	0.00	0.00	0.01	0.01	0.27	0.29	0.35	0.93	0.98	0.98	0.98	0.98	0.98	0.02	0.02	0.34	0.32
Mg/(Ca+Fe+Mg)	0.74	0.74	0.74	0.74	0.74	0.74	0.76	0.76	0.76	0.60	0.57	0.49	0.04	0.01	0.00	0.01	0.00	0.00	0.71	0.71	0.51	0.54
Fe/(Ca+Fe+Mg)	0.26	0.26	0.26	0.26	0.26	0.26	0.23	0.23	0.23	0.13	0.14	0.16	0.03	0.01	0.02	0.00	0.02	0.02	0.27	0.26	0.15	0.15

Table 2: Least squares mixing calculations to approximate the bulk corona composition in terms of the reacting phases olivine and plagioclase. Compare the calculated bulk corona composition with that estimated by mixing of the reactants.

	olivine	plagioclase	bulk symplectite	est. symplectite
SiO2	37.79	51.50	48.13	48.80
TiO2	0.03	0.06	0.09	0.03
Al2O3	0.01	28.49	22.10	21.89
FeO	23.35	0.26	5.67	6.01
MnO	0.45	0.04	0.08	0.12
MgO	37.42	0.00	10.37	9.61
CaO	0.00	12.63	12.20	10.20
Na2O	0.00	4.30	1.24	3.21
K2O	0.00	0.09	0.12	0.04
wt% componant	1	2.97	3.97	Rsqd = 9.16

volumes of components and the likelihood that the orthopyroxene rim partially formed above the solidus in open system reaction (e.g. Johnson and Carlson, 1990) with a liquid phase. However it is important to note that the worst match is that for Na_2O which is significantly lower in the bulk symplectite relative to the estimated symplectite. This provides support for equation 3 and the notion that a potential gradient in Na may have driven symplectite formation. The system must also have been open with respect to H_2O and TiO_2 which do not occur in either reactants. Nevertheless, the calculations show that the products can be broadly accounted for by reacting olivine and plagioclase in the proportions 1:3. This correlates with the symplectite comprising ~71% of the total corona and suggests that the original plagioclase-olivine boundary is represented by the orthopyroxene- or amphibole-symplectite boundary, consistant with the findings of Mongkoltip and Ashworth (1983) that Si and Al are relatively immobile.

In conclusion it can be said that due to the high thermodynamic variance of the corona textures described, phase diagram considerations are difficult to apply. However, from textural evidence we interpret (1) formation of the inner, orthopyroxene corona mantling the olivines close to the solidus and possibly in the presence of magma; (2) formation of the outer, vermicular corona during sub-solidus conditions; (3) formation of the central, incomplete hydrous amphibole/biotite corona during subsequent hydration of the system. The coronas formed in response to compositional gradients (Na and H_2O) during igneous cooling rather than during a subsequent (metamorphic) event.

Acknowledgements

We wish to thank M. Sandiford who first drew attention to the symplectites from Black Hill and their complexities. We also thank M. Sandiford, J. Foden and K. Stewart for thoughtful discussions on their origin and G. Chinner and L. Barron for constructive reviews.

References

Ashworth, J. R. (1986) The role of magmatic reaction, diffusion and annealing in the evolution of coronitic microstructure in troctolitic gabbro from Risör, Norway: a discussion. *Mineral Mag.*, **50**, 469–73.

Blundy, J. D. and Holland, T. J. B. (1990) Calcic amphibole equilibria and a new amphibole–plagioclase geothermometer. *Contrib. Mineral. Petrol.*, **104**, 208–24.

Campbell, I. H. and Nolan, J. (1974) Factors effecting the stability field of Ca-poor pyroxene and the origin of the Ca-poor minimum in Ca-rich pyroxenes from tholeiitic intrusions. *Ibid.*, **48**, 205–19.

Ellis, D. J. (1980) Osumilite-sapphirine-quartz granulites from Enderby Land, Antarctica: P-T conditions of metamorphism, implications for garnet-cordierite equilibria and the evolution of the deep crust. *Ibid.*, **74**, 201–10.

Helz, R. T. (1982) Phase relations and compositions of amphiboles produced in studies of the melting behaviour of rocks. In *Amphiboles: Petrology and Phase Relations* (Veblen, D. R. and Ribbe, P. H., eds.), Min. Soc. Am. Reviews in Mineralogy, **9B**, 279–354.

Joesten, R. (1986*a*) The role of magmatic reaction, diffusion and annealing in the evolution of coronitic microstructure in troctolitic gabbro from Risör, Norway. *Mineral Mag.*, **50**, 441–67.

—— (1986*b*) Reply. *Mineral Mag.*, **50**, 474–9.

Johnson, C. D. and Carlson, W. D. (1990) The origin of olivine-plagioclase coronas in metagabbros from the Adriondack Mountains, New York, *J. Met. Geol.*, **8**, 697–717.

Kushiro, I. (1969) The system forsterite-diopside-silica with and without water at high pressures. *Am. J. Sci.*, **267**, 269–94.

Monkoltip, P., and Ashworth, J. R. (1983) Quantitative estimation of an open system symplectite forming reaction: Restricted diffusion of Al and Si in coronas around olivine. *J. Petrol.*, **24**, 635–61.

Nishiyama, T. (1983) Steady state diffusion model for olivine–plagioclase corona growth. *Geochim. Cosmochim. Acta.*, **47**, 283–94.

Turner, S. P. (1992) Petrology of Late-orogenic layered gabbros, potassic monzonites and A-type granophyres from Black Hill, South Australia. *J. Petrol.* (submitted).

van Lamoen, H. (1979) Coronas in olivine gabbros and iron ores from Susimäki and Riuttamaa, Finland. *Contrib. Mineral. Petrol.*, **68**, 259–68.

[*Manuscript received 15 July 1991: revised 17 March 1992*]